2007 IEEE International Conference on
Robotics and Automation
Roma, Italy, 10-14 April 2007

Application of Electronic Compass for Mobile Robot in an Indoor Environment

Vladimir Y. Skvortzov, *Member, IEEE,* Hyoung-Ki Lee, SeokWon Bang and YongBeom Lee

***Abstract*—This paper presents a novel approach to electronic compassing for robot in an indoor environment. Operation of compass (magnetometer) is assumed on a mobile robot that is capable to traverse a complete circular path. The electronic compass is used to estimate a robot absolute heading with respect to the magnetic North. This is only compass approach where an evaluation of quality of calibration and magnetic environment is important as much as calibration itself. In this method, compass is able to detect the external magnetic interference and estimate it numerically. The approach also relates to automatic calibration and requires one full 360-degree rotation and multiple points for further analysis. This enhanced calibration procedure is performed in the magnetic field domain and implemented using a non-iterative algebraic technique. The quality of calibration is a function of input data goodness and how successful is the fitting procedure. The magnetic environment evaluation is performed by the distortion factor that is calculated at the end of calibration and helps to estimate quantitatively local external magnetic distortions and their influence on a heading measurement. The validity of this approach has been verified experimentally by using robot with electronic compass.**

I. INTRODUCTION

Electronic compasses are widely used in modern applications. Many vehicles, including vehicles used by consumers have built-in compasses.

An electronic compass is a device that indicates the yaw heading to an object by measuring the earth's magnetic field. If the compass is built into a vehicle, the compass may simply indicate the direction the vehicle is headed. In minimal configuration the output from two of magnetometers mounted at right angles to each other is used to compute the direction of the horizontal component of the Earth's magnetic field.

In spite of some problems due to magnetic interferences, compasses have become more popular in indoor robotic applications. However, those problems still have to be solved.

Manuscript received September 15, 2006.

V. Y. Skvortzov is with the Advanced Systems Research Lab, Samsung Advanced Institute of Technology, Yongin-Si, Kyungki-Do 449712 South Korea (corresponding author phone: +82 031-280-6538; fax: +82 031-280-9208; e-mail: v.skvortzov@samsung.com).

H.-K. Lee is with the Advanced Systems Research Lab, Samsung Advanced Institute of Technology, Yongin-Si, Kyungki-Do 449712 South Korea (e-mail: twinclee@samsung.com).

S.-W. Bang is with the Advanced Systems Research Lab, Samsung Advanced Institute of Technology, Yongin-Si, Kyungki-Do 449712 South Korea (e-mail: banggar.bang@samsung.com).

Y.-B. Lee is with the Advanced Systems Research Lab, Samsung Advanced Institute of Technology, Yongin-Si, Kyungki-Do 449712 South Korea (e-mail: leey@samsung.com).

II. REVIEW & DISCUSSION

Every compass on a vehicle will suffer from local deviation effects, due to local magnetic interferences such as site magnetic anomalies, cabling, the electrical motors, batteries and boards – almost any ferrous or magnetic object. Since the Earth's magnetic field is weak and metal objects distort that field, one must calibrate the output of an electronic compass to achieve reasonably accurate results.

If the magnetic interference from compass host platform is constant, it can effectively be compensated.

The traditional compass calibration involves placing the compass on a mechanical device that rotates the compass to known orientations. If the compass is disposed in a vehicle, this involves moving the vehicle (and its compass) in a circle. The compass output is recorded and compared against a known orientation, calculating corrections to the compass measurements (more detailed description is in [1]). While this method is effective, it is laborious and slow task [2].

However, some on-board magnetic interferences are variable. Mainly they come from the electrical motors. The well-known solution is a shielding [1], which can be enough effective. Recognizing a profit of the shielding, in our experiments we have found that variable interferences of electrical motors are not main contribution factor to deviation caused by the host platform. The effect of variable interferences of motors is significantly reduced simply placing a compass as far as possible from the motors.

Tilting an electronic compass can create heading errors. However we do not consider that in this paper, since many researchers have already done it as in [3]-[4].

Indoor operation of wheeled robot with compass has some features. A human-built indoor environment has a lot of sources of magnetic interference such as reinforced concrete structures (floor and walls), pipes, built-in cabling, wiring and different metal and magnetic objects. If a height of compass location above the floor is low, the compass experiences a magnetic interference from floor fields which may be stronger then one that comes from host platform.

The fundamental problem of compass navigation and orientation in an indoor environment is a deviation produced by external magnetic interference. The amount and direction of the magnetic interference is unpredictable and cannot be modeled numerically or compensated through calibration. Such external magnetic interferences may dramatically increase errors in compass. Application of the common Kalman

Filter approach has not produced a satisfactory answer ([1], [5]) to the problem because the difficulty of modeling external magnetic interference.

Although external magnetic interference cannot be compensated, there are some properties of magnetic fields that can be used to detect the interference. In that case, at least the user will know if the compass readings are correct or not.

In known publications most authors ([1], [5], [6]) consider two practical methods for detecting such magnetic disturbances: redundant sensors [5] (typical example of this method is a gyro-aided compass) and differential compass [6].

A major problem with the gyro-aided compass method ([7], [8]) is the requirement of a pre-calibrated heading rate gyro. Moreover, the gyro due to inherent bias drift problems has to be recalibrated more often than the compass.

The differential compass approach increases cost of the system and also may have problems with magnetic interference.

We propose alternative method that uses only compass to detect the interference and estimate it numerically. To the best of our knowledge this method has not been suggested before.

It is known fact that locus (or *x*-*y* plot) of raw data from two perpendicularly mounted magnetometers has ellipse-like shape because of various magnetic distortions and distortion-free measurement gives a circle. Probability of event that distorted data give a locus close to circle shape is negligible small. The locus already contains some detectable signs of external interference and those can be extracted using different data analysis techniques.

After analysis of different calibration methods we have found that so called magnetometer-based approach is enough effective because raw magnetometer data is directly corrected, eliminating the need for a compass error model.

In addition, an optimal combination of higher sampling rate and calibration quick rotational motion can dramatically improve a speed of calibration, reducing a need for smaller number of calibration points to perform fast. The calibration operation can now be done in 5 seconds or less if a rotational robot speed is about 80 deg/s. The present approach provides a fast, automated solution to the problem of application of an electronic compass for mobile robot and allows evaluating local magnetic distortions without using additional sensors.

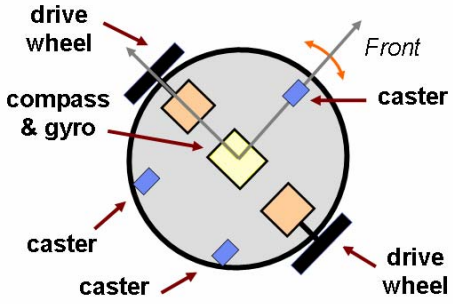

Fig. 1. Scheme of mobile robot (top view) with compass and gyro (for verification of compass measurements).

The robot chassis used in our experiments is the vehicle (Fig. 1) with differential steering - two individually controlled drive wheels on each side of base with casters in front and rear for stability. Such configuration allows the robot to spin in place about vertical axis. Our approach is also applicable to car-like robot, when it is driven in a complete circle. However, it is evident that car-like steering configuration gives less satisfactory results than differential steering one.

III. Compass Data Processing

A. Approach

As a rule, multiple (x, y) points must be acquired to properly calibrate the compass. The points are collected in a loop; and an algorithm can be coded so the loop stops when condition of the end becomes true. A requirement for using this algorithm is that the vehicle is rotated through one complete circle, so that there is an equal representation of magnetometer readings in all directions. A calibration procedure must provide the compass with all 360 degrees of direction as well maintaining an equal amount of samples from each direction. An unequal number of samples in all directions may result in poor performance. Also true, if calibration does not expose the compass to all 360 degrees, will result in poor performance.

We focus on static compass measurements of robot orientation because it gives more stable and proper results. Our approach is a synergy of three important procedures: calibration, evaluation of its quality, and detection of magnetic interference with its numerical evaluation.

Consider a local level magnetometer data set:

$$\begin{bmatrix} X_{\mathbf{r}} \\ Y_{\mathbf{r}} \end{bmatrix} = \begin{bmatrix} x_{r1} & x_{r2} & \dots & x_{rn} \\ y_{r1} & y_{r2} & \dots & y_{rn} \end{bmatrix},$$

where $\mathbf{X_r}$ and $\mathbf{Y_r}$ are magnetometer raw data sets for x and y axes respectively, and n is a number of points.

After acquisition phase of the calibration has been done, one can build a graph of the data. Fig. 2 shows a typical graph of all the points acquired in an indoor environment. The graph is elliptical with the major axis approximately along the X. The elliptical figure is due to the X values having a greater gain than the Y values and soft iron effects. The center of the ellipse is also off the origin.

Hard iron error is first characterized by identifying the location of the center of the circle (or ellipse if soft iron errors are present). One of variants is simply done by taking the average of $\mathbf{X_r}$ and $\mathbf{Y_r}$ measurement sets, as proposed in [2]:

$$x_h = \frac{1}{n}\sum_{i=1}^{n} x_{ri}, \quad y_h = \frac{1}{n}\sum_{i=1}^{n} y_{ri}$$

where (x_h, y_h) are hard iron offsets for x and y.

Another variant is to compute the calibration values based on the maximum and minimum X and Y values acquired. These values can later be used to correct the raw X and Y values acquired when computing the heading.

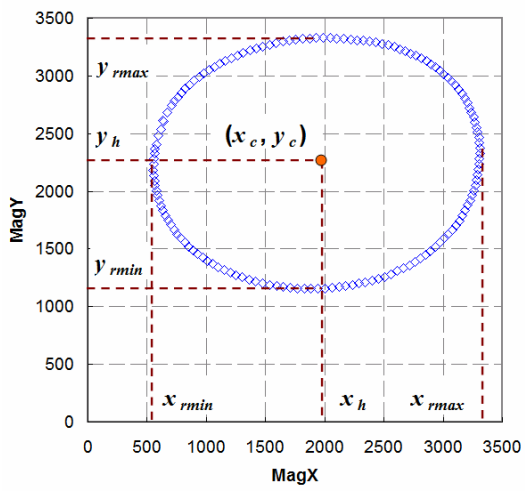

Fig. 2. Raw data points for calibration; (x_c, y_c) – coordinates of estimated center.

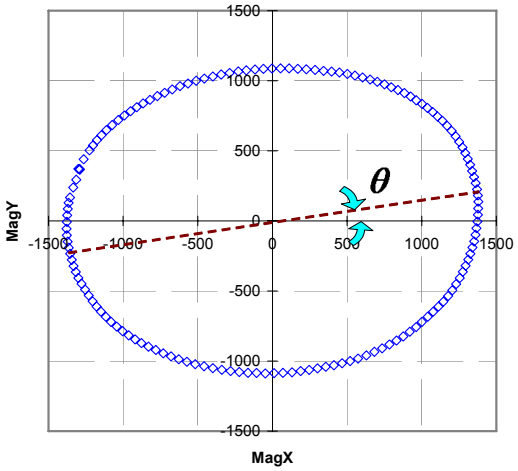

Fig. 3. Data after hard iron correction.

The raw data offsets can be very effectively eliminated by using a simple subtraction technique. First, one may calculate offsets

$$x_h = (x_{rmax} + x_{rmin})/2, \quad y_h = (y_{rmax} + y_{rmin})/2,$$

where (x_{rmax}, y_{rmax}) and (x_{rmin}, y_{rmin}) are maximum and minimum values of $\mathbf{X_r}$ and $\mathbf{Y_r}$ sets respectively.

To obtain the correct heading a graph of the points (x, y) should show a circle or ellipse with the center in the origin. In first, it is necessary to subtract out the offsets

$$\begin{bmatrix} X_{rh} \\ Y_{rh} \end{bmatrix} = \begin{bmatrix} X_r - x_h \\ Y_r - y_h \end{bmatrix}.$$

Fig. 3 shows how the raw (x, y) points are corrected using the calibration values to get the figure at the origin.

With the *hard iron* error subtracted out, *soft iron* errors are now characterized by the *angle of the major axis* (Fig. 3, θ) of the elliptical magnetometer plot (with respect to North) and the *ratio of the major axis to the minor axis lengths*. One of techniques to remove the soft iron effect is to rotate the reading by $-\theta$ (actual angle sign is determined by direction clockwise (CW) or counterclockwise (CCW); in general we have to rotate data in direction that is opposite to current), scale the major axis to change the ellipse to a circle, and then rotate the reading back by θ.

There are different ways how to find the θ. It is known fact that the angle of the major axis of the ellipse corresponds to the least second moment of inertia. This is found using the following equation

$$\theta_{MI} = 0.5 \cdot \tan^{-1}\left[\left(2 \cdot U_{xy}\right) / \left(U_{xx} - U_{yy}\right)\right], \qquad (1)$$

where U_{xx}, U_{yy}, and U_{xy}, are the second order *x*-axis, *y*-axis, and mixed moments, respectively and θ_{MI} is the angle calculated by moment of inertia and measured in a +CW manner with respect to the +X axis. These moments are computed

$$U_{xx} = \frac{1}{n}\sum_{i=1}^{n}\left(x_{ri} - x_h\right)^2, \qquad (2)$$

$$U_{yy} = \frac{1}{n}\sum_{i=1}^{n}\left(y_{ri} - y_h\right)^2, \qquad (3)$$

$$U_{xy} = \frac{1}{n}\sum_{i=1}^{n}\left(x_{ri} - x_h\right)\left(y_{ri} - y_h\right). \qquad (4)$$

Moment of inertia is the name given to rotational inertia, the rotational analog of mass for linear motion. For a point mass the moment of inertia is just the mass times the square of perpendicular distance to the rotation axis. To use the moment of inertia one can also consider ellipse-like magnetometer points as collection of point masses.

There are some issues with (1). In first it is sensitive to data offset. Another issue is related to robot rotation, when it starts and stops at the same point doing complete circular path, having the constant data-sampling rate, one cannot have equal representation of points in all directions because of acceleration and deceleration it is not rotated at constant speed during the move. Equation (1) is also sensitive to unequal distribution of data, and in such cases it can give angle (θ_{MI}) with error so that removing offset and filtering are required.

Another way to find the θ angle and all other parameters is to fit an ellipse to scattered magnetometer data, obtain an ellipse polynomial equation and calculate the parameters. The "fitting an ellipse to data" method eliminates creating of two fitting models of *X* and *Y* sets that makes modeling easier. The ellipse fitting divides into two broad techniques: clustering and least-squares fitting. Least-squares techniques center on finding the set of parameters that minimize some distance measure between the data points and the ellipse.

A general form of conic equation in arbitrary position can be written by an implicit second order polynomial (an ellipse is a type of conic section):

$$\mathrm{F}(\mathbf{a}, \mathbf{x}) = \mathbf{a} \cdot \mathbf{x} = a \cdot \mathrm{x}^2 + b \cdot \mathrm{x} \cdot \mathrm{y} + c \cdot \mathrm{y}^2 + d \cdot \mathrm{x} + e \cdot \mathrm{y} + f = 0, \qquad (5)$$

where $\mathbf{a} = [a\ b\ c\ d\ e\ f]^T$ is the parameter vector and $\mathbf{x} = [x^2\ xy\ y^2\ x\ y\ 1]^T$. $F(\mathbf{a}; \mathbf{x}_i)$ is the 'algebraic distance' of a point (x, y) to the conic $F(\mathbf{a}; \mathbf{x}) = 0$. The fitting of a general conic may be approached by minimizing the sum of squared algebraic distances

$$D_A(\mathbf{a}) = \sum_{i=1}^{N} F(\mathbf{x}_i)^2 \qquad (6)$$

of the curve to the N data points $\mathbf{x}_i$. In order to avoid the trivial solution $\mathbf{a} = 0_6$, and recognizing that any multiple of a solution a represents the same conic, the parameter vector **a** is constrained in some way. Many of the published algorithms differ only in the form of constraint applied to the parameters. There is more detailed discussion on the topic in [11]. We select a quadratic constraint in form of $\mathbf{a}^T\mathbf{C}\mathbf{a} = 1$ where **C** is a 6×6 constraint matrix. If a quadratic constraint is set on the parameters the minimization (6) can be solved by considering rank-deficient generalized eigenvalue system:

$$\mathbf{D}^T\mathbf{D}\mathbf{a} = \lambda\mathbf{C}\mathbf{a},$$

where $\mathbf{D} = [x_1\ x_2\ \dots\ x_n]^T$ is the design matrix.

Many methods of ellipse fitting rely either on generic conic fitting or on iterative methods to find the estimation towards ellipticity. Iterative methods are computationally expensive, difficult to implement.

In [10] authors have developed a non-linear two-step estimator to least-square technique for calibration algorithm of solid-state strapdown magnetometers. That idea is close to iterative techniques as well.

In [9] authors have shown a new method of direct ellipse-specific fitting while retaining the efficiency of solution of the linear least-squares problem (6) where the parameter vector **a** is constrained so that the conic that it represents is forced to be an ellipse. The solution is the equality constraint $4ac - b^2 = 1$.

Finally, the constrained ellipse fitting problem reduces to minimizing $E = \|\mathbf{D}\mathbf{a}\|^2$ subject to the constraint $\mathbf{a}^T\mathbf{C}\mathbf{a} = 1$.

Introducing the Lagrange multiplier λ and differentiating, we obtain the system of simultaneous equations

$$\begin{cases} 2\mathbf{D}^T\mathbf{D}\mathbf{a} - 2\lambda\mathbf{C}\mathbf{a} = 0 \\ \mathbf{a}^T\mathbf{C}\mathbf{a} = 1 \end{cases}$$

This may be rewritten as the system

$$\mathbf{S}\mathbf{a} = \lambda\mathbf{C}\mathbf{a} \qquad (7)$$
$$\mathbf{a}^T\mathbf{C}\mathbf{a} = 1$$

where **S** is the scatter matrix $\mathbf{D}^T\mathbf{D}$. This system is readily solved by considering the generalized eigenvectors of (7) [9].

After finding solution and parameters of equation (5), the center of the ellipse with help of fitting is (x_{fc}, y_{fc}), where

$$x_{fc} = (cd - bf)/(b^2 - ac), \quad y_{fc} = (af - bd)/(b^2 - ac).$$

The base form of semi-axis length equation is as follows

$$S = \sqrt{\frac{2(af^2 + cd^2 + gb^2 - 2bdf - acg)}{(b^2 - ac)\left[M\sqrt{1 + (4b^2/(a-c)^2)} - (c+a)\right]}}$$

and finally the two semi-axes lengths are $S_1 = S$, where $M = c - a$ and $S_2 = S$, where $M = a - c$.

The angle of rotation with help of fitting is (CCW rotation is positive)

$$\theta_F = 0.5 \cdot \arctan((2b)/(c-a)). \qquad (8)$$

Final selection of the θ reduces to choice between θ_{MI} and θ_F. The way with help of fitting is more stable than using (1) but it can hide some input data issues (we can fit ellipse to almost any scattered data). In addition, in some situations a higher sensitivity to input data of the θ_{MI} can play a positive role, for example, when properly used it can indicate local distortions of data. Although in theory we could expect that both techniques always must give the same result, it is not true at practice.

After selection of calculation method and with the major axis angle known, the hard iron calibrated magnetometer data set is rotated about the origin by the angle $-\theta$ so that the major axis lies along the x+ axis

$$\begin{bmatrix} X_{rot1} \\ Y_{rot1} \end{bmatrix} = \begin{bmatrix} \cos(-\theta) & -\sin(-\theta) \\ \sin(-\theta) & \cos(-\theta) \end{bmatrix} \begin{bmatrix} X_{rh} \\ Y_{rh} \end{bmatrix}.$$

Then the ranges of the data are shown in Fig. 2 and found

$$x_{rrange} = (x_{rmax} - x_{rmin}),\ y_{rrange} = (y_{rmax} - y_{rmin}). \qquad (4)$$

The scale conversion factor s is then determined, if $x_{rrange} > y_{rrange}$ then $s = x_{rrange}/y_{rrange}$ and, if $y_{rrange} \geq x_{rrange}$ - $s = y_{rrange}/x_{rrange}$.

With θ and s known, the magnetometer reading can be calibrated by rotating the reading by $-\theta$, scaling the minor axis component by s, and then rotating the reading back to it's original orientation

$$\begin{bmatrix} X_{cal} \\ Y_{cal} \end{bmatrix} = \mathbf{A} \cdot \mathbf{B},$$

where $\mathbf{A} = \begin{bmatrix} \cos(\theta) & -\sin(\theta) \\ \sin(\theta) & \cos(\theta) \end{bmatrix} \begin{bmatrix} 1 & 0 \\ 0 & s \end{bmatrix}$ (for $x_{rrange} > y_{rrange}$),

$$\mathbf{B} = \begin{bmatrix} \cos(-\theta) & -\sin(-\theta) \\ \sin(-\theta) & \cos(-\theta) \end{bmatrix} \begin{bmatrix} X_{rh} \\ Y_{rh} \end{bmatrix}.$$

Fig. 4 shows the plot of the corrected X, Y points (marked as MagY Rot2) using the calibration values. The offsets move the center of the figure back to the origin and the ranges are used to match the gain so the graph will become more close to circle from the original ellipse-like figure.

Finally we can compute an angle in degrees

$$angle = \arctan(y_{cal}/x_{cal}) \cdot (180/\pi), \qquad (9)$$

where (x_{cal}, y_{cal}) are x and y calibrated values.

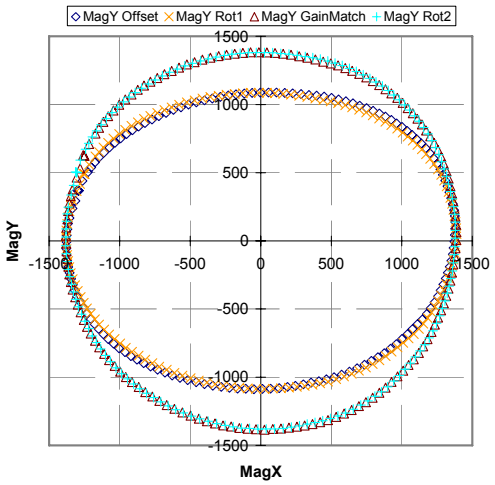

Fig. 4. Calibration stages: after removing offset (MagY Offset), 1st rotation (MagY Rot1), gain match (MagY GainMatch), and final result after 2nd rotation (MagY Rot2).

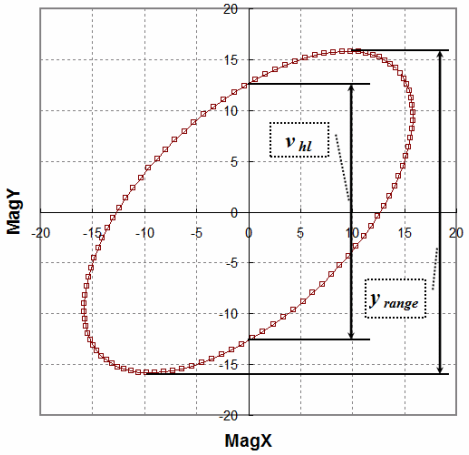

Fig. 5. Lissajous method for phase shift determination.

Equation (9) uses arctangent function. Since the arctangent result is only in the range of 0 to 90, care is needed to take note of the sign of X and Y to determine the correct quadrant and to add the proper padding to determine a heading.

In numerical library of many programming languages, there is a two-parameter **atan2(y, x)** function that returns *angle*, measured in radians, such that $-\pi \le angle \le \pi$, using the signs of the parameters to find the quadrant, and tan(*angle*) = y / x, where (x, y) is a point in plane.

B. Data Analysis

For the data analysis is necessary to calculate some parameters which can be helpful in addition to θ. Let us define those parameters.

1) Some Parameters

Circularity is a measurement of the ratio of the actual perimeter of a particle to the perimeter of a circle with the same area as the particle. Circularity also has values in the range 0-1. A perfect circle has a circularity of 1 while a very 'spiky' or irregular object has circularity closer to 0. Intuitively circularity is a measurement of irregularity or difference from a perfect circle. This parameter may especially be helpful for evaluation how successful is calibration (how close is final calibrated locus shape to circle). It is less practical for evaluation of raw data because of its sensitivity to input data noise. The value is computed as

$$R_c = P \Big/ \left(2\sqrt{\pi A}\right). \qquad (10)$$

where P – data perimeter, A – data area.

A phase shift between X and Y is a good measure of distortions. One of the methods for determining the phase difference between two signals at the same frequency is called Lissajous figures. By examining the original plot of the two X and Y traces versus time, one can determine the relative phase shift φ. In this case, the signals are not plotted versus time, but rather one versus the other (Fig. 5). A signal must be centered in X-axis and the phase shift φ in degrees is:

$$\varphi = \arcsin\left(v_{hl} / y_{range}\right) \cdot (180/\pi), \qquad (11)$$

where v_{hl} – distance between 2 points of intersection of ellipse with Y-axis , y_{range} – Y-axis range of fitted ellipse data.

2) Quality of calibration

The quality of calibration may include parameters of input data quality and fitting quality. If the data are sufficient for proper evaluation, the input data quality shows how they are equally distributed in circle. Here we define the quality of calibration as an average of included parameters.

We can evaluate how equally data are represented in all directions by following coefficient of maximum difference (irregularity)

$$C_{md} = \left[\left(\max_{i=1}^{4}\left(\left|\mathrm{num}(i)\right|\right) - \min_{i=1}^{4}\left(\left|\mathrm{num}(i)\right|\right)\right) \Big/ \sum_{i=1}^{4}\left|\mathrm{num}(i)\right|\right] \cdot 100,$$

where **num** = [*numI numII numIII num IV*], *numI* – number of points in I quadrant and etc. The number of points in each of 4 quadrants is a simplified measure to evaluate how equally magnetometer readings are represented in the quadrants. To use equation above offset removal is required.

A ratio of raw data and fitted ellipse area is related to quality of fitting

$$R_{rf} = A_r / A_f ,$$

where A_r – raw data area, A_f – area of fitted ellipse.

The quality of calibration includes raw data and fitting goodness. The R-squared value (R_{sq}) is a measure of the fitting goodness and is the square of the correlation coefficient that is a ratio of variations between the variables estimated using the fit equation and the actual variables. The measure is defined as

$$R_{sq} = \sum_{i=1}^{n}\left(Y_{fi} - y_{fmean}\right)^2 \Big/ \sum_{i=1}^{n}\left(Y_{ri} - y_{rmean}\right)^2 ,$$

where $\mathbf{Y_f}$ – filtered set of values of fitted ellipse from (5) using the same input X-values, y_{fmean} – mean value of $\mathbf{Y_f}$, y_{rmean} – mean value of $\mathbf{Y_r}$. The closer the R_{sq} value is to 1, the better the equation fits the underlying data.

A ratio of standard deviation of magnetic field density to

mean of the magnetic field density is written as

$$R_{sm} = S_{mfd} / M_{mfd},$$

where S_{mfd} – the standard deviation of magnetic field density, M_{mfd} – mean of magnetic field density of n points after removing offset. This parameter allows to evaluate data spread of magnetic field density during the calibration. The horizontal component of magnetic field density is $B_h = \sqrt{x_{rh}^2 + y_{rh}^2}$, where ($x_{rh}$, y_{rh}) – raw data point after removing hard iron offset.

Finally the quality of calibration in % is

$$QC = \text{Average}((100 - C_{md}) + R_{rf} \cdot 100 + \\ + R_{sq} \cdot 100 + (100 - R_{sm} \cdot 100)). \quad (12)$$

For comprehensive analysis, the QC may be improved by addition of the circularity R_c by (10) which can be considered separately of QC as well and ratio of moments (2)-(4) for raw and fitted data.

3) Distortion factor

An idea behind introduction of distortion factor is an approximate evaluation on how heavily magnetic anomalies have distorted compass measurements. The higher distortions mean higher distortion factor. In this context, the factor has to accumulate various distortions found during the raw data analysis. The distortion factor is defined as

$$DF = \theta_{MI} \cdot w_1 \cdot (1 - (C_{md} / 100)) + \\ + (90 - \varphi) \cdot w_2 + \theta_F \cdot w_3 + C, \quad (13)$$

where θ_{MI} – angle in (1), φ – phase shift in (11), θ_F – angle in (8), w_1, w_2, w_3 – empirical weight coefficients for each corresponding term, and C – constant.

A general rule for selection of C is the C must have such value so that not distorted measurements will always give zero value or value close to zero. To find rational values of the weight factors and C some experiments are required. Once we set the C value and weight factors, we have to use it to make our data comparable for analysis. Introducing C_{md} into (13), we want to control effect of θ_{MI} and make it dependent on input data quality. Unit of measurement for the DF is degree because all members of (13) are angles in degrees.

C. Algorithm and software

In Fig. 6, *a* is shown the simplified flow chart of the algorithm. The algorithm starts with raw data collection and pre-processing. The data are one-dimensional arrays of X and Y magnetometer readings.

For accurate calibration more then 100 points in complete 360-degree rotation are recommended, otherwise some essential information of raw data shape (equals magnetic distortions) can be lost. The calibration may be executed at any reasonable speed to meet the 100 points requirement. For example, at condition of robot rotational speed 80 deg/s (corresponds to robot linear speed of 20 cm/s) and compass sampling rate 33 Hz, we can obtain about 148 points.

It is strongly recommended to filter the data before use because it may contain different kinds of wrong information as data acquisition failures, outliers, unexpected spikes and other redundant data. It is first stage of filtering. To follow the rule of equal representation of magnetometer readings in all directions and remove redundant points we have to find a number of points in 4 quadrants (**num**) and C_{md}. For filtering we select simple filter that calculates Euclidean distances between points, checks a number of points in 4 quadrants and removes every point of 2 points if the distance is less then the specified threshold, for example, 75% of mean distance (those points are located too close to each other, when data collection at low speed or at stop) at conditions of reducing C_{md} and having more than 100 points after the filtering.

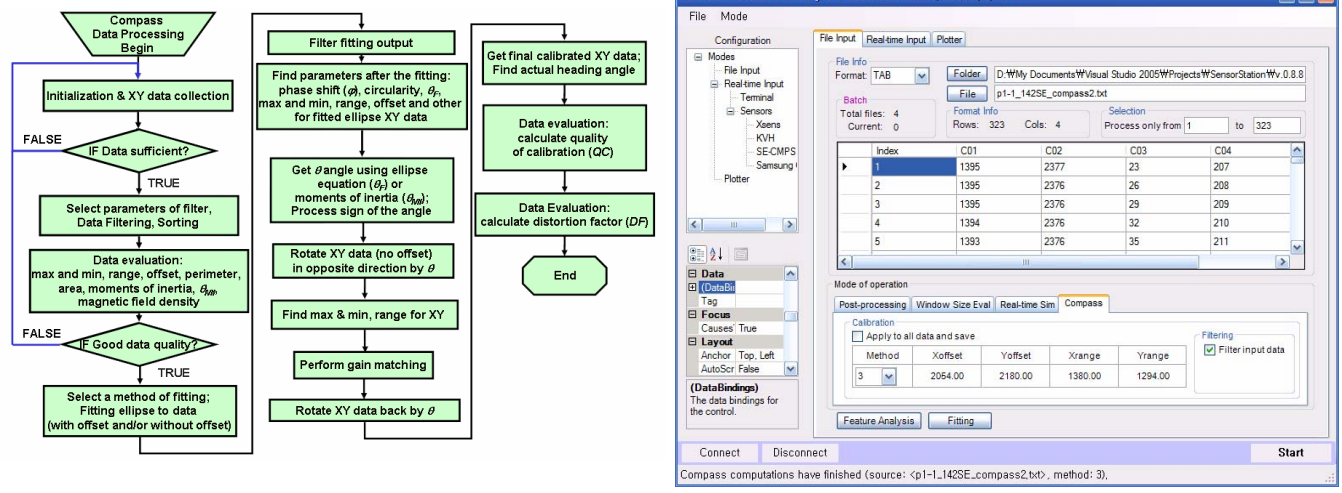

a *b*

Fig. 6. (*a*) Algorithm simplified flow chart, and (*b*) main window screenshot of the "*SensorStation*" software for compass data acquisition and processing.

In most cases, we need to iterate through this routine several times until all redundant points are removed. In addition, it may be convenient for some processing routines to have the data sorted (data integration is done in more logical way if we have arranged the ellipse data dividing it into top and bottom points and sorted them).

Then we calculate some raw data parameters: perimeter (P_r) and area (A_r). The raw data area is a part of component for estimation of quality of calibration. There are two ways to find raw data area: using Surveyor's formula and integration. If the integration is based on approximate techniques as a trapezoidal rule, in the most cases they give similar results.

In next, it is necessary to remove offset from the data and store resulting data separately for further processing. After offset removal we can find moments of inertia by (2)–(4) and calculate θ_{MI} by (1).

Before applying fitting routines, there is a check of the number of points. For the fitting procedure itself at least 6 points are required, however there is higher-level requirement above that superimposes on this one.

In beginning, a selection of fitting method is required, then populating the design (**D**) and constraint (**C**) matrices to find the scatter matrix **S**. The solution uses algebraic approach to constrained least-squares fit of an ellipse to data.

The result of the fitting is the parameter vector **a** with the coefficients of (5). Having the parameters, we can do analysis of the data. We can calculate the *QC* using (12). Finally, we can find the distortion factor by (13).

Most of calculations in this paper were made using custom software (Fig. 6, *b*) written in Microsoft® Visual C# .NET 2005. The software has the following system requirements: MS Windows 98, .NET Framework v.2.0 redistributable package, 600 MHz Pentium® processor or higher, RAM - 192 MB, disk space - 3.5 MB (without Framework), display - 800 × 600 256 colors. The software uses multi-threading, generics and inheritance to take full advantage of built-in technologies of object-oriented programming. Processing about 300 compass points takes about 1 s using Pentium 4 3 GHz processor. The algorithm can be implemented on mobile hardware.

IV. Experiments

The compass used in the experiments described throughout this paper is the GMCS GCS002IA fluxgate compass made by Samsung Electro-Mechanics [11]. The compass was installed on robot front side about 10 cm above floor (Fig. 7). Data from compass were verified by gyro measurements.

In first series of experiments, we tested a feasibility of our approach. All experiments were carried out in random sites of typical office environment. With fixed start compass orientation about 142° SE (South-East), the compass has been rotated through 360 degrees by mobile robot with speed of 80 deg/s and data sampling rate 33 Hz. Also we did measurements with different start orientations helped to identify 'start point' issue mentioned in comments to (1) in *Section III.A*. Results of the experiments with the fixed orientation are presented in Fig. 9, *a*. Another goal was to check different combinations of weight factors for *DF* in (13). For data analysis we used the following combination: $w_1 = 1$, $w_2 = 0.7$, $w_3 = 0.3$, $C = 15$; C_{md} excluded. That combination is not optimal; it gives more priority to θ_{MI} known by high sensitivity to data. In spite of that we can observe that more externally distorted measurements give higher number of distortion factor.

For final experiments, a typical living room in apartment was modeled with some consumer electronics to evaluate their influence on compass data – those are sources of magnetic disturbances such as refrigerator, TV, speakers of audio system (Fig. 8). A distance between fridge, TV, speaker and test points was about 40 cm. At each point compass data measurements were made two times for fixed start compass orientation that is about 142° SE. Alternative measurements were carried out at some height (to avoid an influence of magnetic disturbances from floor and others) with needle compass to validate the data from electronic compass. The compass has been rotated in the same way as in first experiments. At post-processing, the data were filtered and processed according to the algorithm in *Section III.C* to obtain calibration parameters, *QC* and *DF*. The *DF* calculated with the empirical coefficients as $w_1 = 0.05$, $w_2 = 0.1$, $w_3 = 0.1$, $C = -9$ and Abs(θ_F) (Fig. 9, *b*).

Errors during the measurements are induced by initial orientation misalignment error, robot command execution errors. There is some influence of data filtering on final results too.

Based on the data one can make some conclusions that approximately 88% points of 17 (15 points of 17), where heading angle is 142±10°, are within $-3.3 \le DF \le 3.5$ - the area is shown as dashed rectangle in Fig. 9, *b*. In spite of some points are out of the limits, the experiments are clear proof of practical value of the distortion factor parameter.

V. Conclusions

Problems of compass application for mobile robot in an indoor environment have been investigated. The variation in heading angle in our experiments due to external magnetic interference was about ±30° and may be higher. Finding a solution to this problem is one of the challenges faced by developers today.

This paper discussed technique to improve a robustness of compass measurements for mobile robot. Our proposed technique uses a calibration, evaluation of quality of the calibration, and evaluation of magnetic environment by the distortion factor. We have built a prototype of robot with electronic compass module and have verified the validity of this approach.

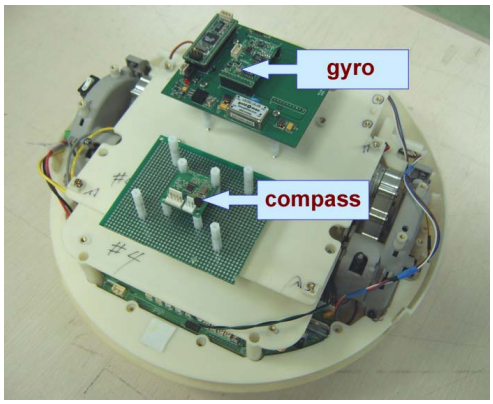

Fig. 7. Mobile robot (prototype of robotic vacuum cleaner) with compass and gyro.

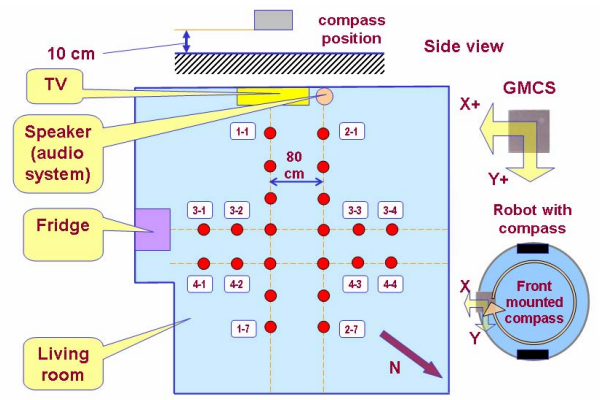

Fig. 8. Experiment scheme (lab's modeled room, top view, test points with identificators).

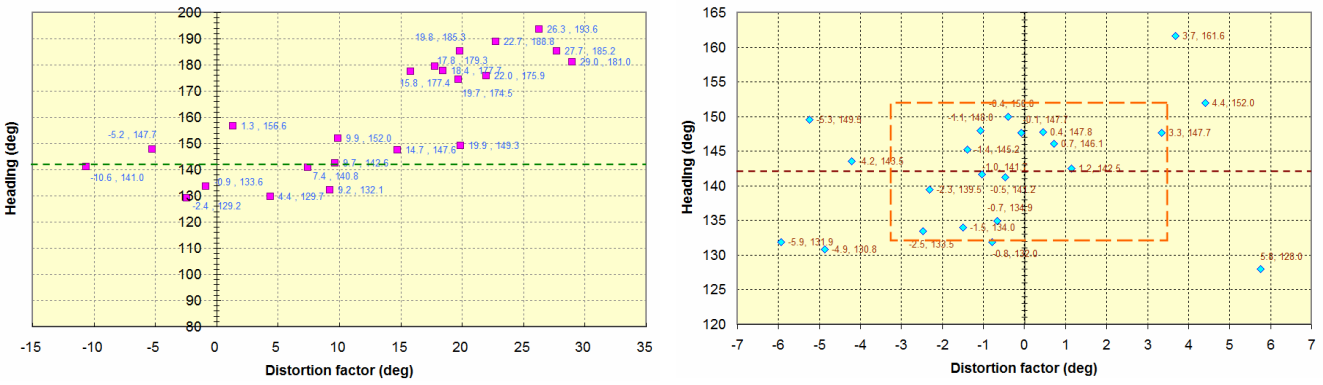

a *b*

Fig. 9. Distortion factor versus heading angle: 22 data points collected as (*a*) experiments in office ($w_1 = 1$, $w_2 = 0.7$, $w_3 = 0.3$, $C = 15$; C_{md} excluded) and (*b*) experiments in the lab's modeled room ($w_1 = 0.05$, $w_2 = 0.1$, $w_3 = 1$, $C = -9$ and Abs(θ_F)).

The distortion factor is a good indicator of magnetic anomalies, which can be used to determine the quality of the compass heading information. Advantage of the approach is that not only we can detect magnetic distortions but also evaluate approximately how heavy they are. With help of such technique at least we can exclude badly distorted data from our measurements. However we have to use it with care because magnetic disturbances are non-linear and may be a result of multiple magnetic sources.

Compass used in the experiments is low cost model and for future work we believe that more precise compass may improve accuracy of the algorithm and prediction capabilities of the distortion factor parameter. In addition, a more sophisticated filtering of input data or providing a constant calibration speed can be a great help as well.

ACKNOWLEDGMENT

Authors thank to Choi Kiwan, Kim DongJo and Park JiYoung of Advanced Systems Research Lab for their help in the compass testing and data collection.

REFERENCES

[1] L. Ojeda and J. Borenstein, "Experimental Results with the KVH C-100 Fluxgate Compass in Mobile Robots," *Proceedings of the IASTED International Conference on Robotics and Applications 2000*, August 14-16, 2000 – Honolulu, Hawaii, USA.

[2] J. J. Mach, "Toward Auto-Calibration of Navigation Sensors for Miniature Autonomous Underwater Vehicles", M.S. thesis (for Master of Science in Electrical Engineering), Blacksburg, Virginia, 2003.

[3] J. Miller , "Mini Rover 7 Electronic Compassing for Mobile Robotics," *CIRCUIT CELLAR*, Issue 165 April 2004, pp.14-22.

[4] S. Y. Cho and C. G. Park, "Tilt compensation algorithm for 2-axis magnetic compass," *ELECTRONICS LETTERS*, 30th October 2003 Vol. 39 No. 22, 2003.

[5] W. Kwon, K.-S. Roh, and H.-K. Sung, "Particle Filter-based Heading Estimation using Magnetic Compasses for Mobile Robot Navigation," *Proceedings of the 2006 IEEE International Conference on Robotics and Automation*, Orlando, Florida - May 2006.

[6] K.-M. Lee, Y.-H. Kim, J.-M. Yun and J.-M. Lee, "Magnetic-interference-free dual-electric compass," *Sensors and Actuators A: Physical*, Volume 120, Issue 2, 17 May 2005, Pages 441-450.

[7] R. T. Azuma, "Calibrating a magnetic compass with an angular rate gyroscope and a global positioning system receiver," U.S. Patent 6408251, June 18, 2002.

[8] R. W. Levi and R. R. Marshall, "Gyro aided magnetic compass," U.S. Patent 6842991, January 18, 2005.

[9] A. W. Fitzgibbon, M. Pilu, and R. B. Fisher, "Direct least-squares fitting of ellipses," *IEEE Transactions on Pattern Analysis and Machine Intelligence*, 21(5), 476--480, May 1999.

[10] D. Gebre-Egziabher, G. H. Elkaim, J. D. Powell, and B. W. Parkinson, "A Non-Linear, Two-Step Estimation Algorithm For Calibrating Solid-State Strapdown Magnetometers," in *Proceedings of The International Conference on Integrated Navigation Systems*, St. Petersburg Russia, May 2001.

[11] Ultra Compact, Dual Axis Electronic Compass with Digital Azimuth Output, Specification Sheet for Geo Magnetic Compass Sensor (GMCS), model GCS002IA, Samsung Electro-Mechanics Co. (SEMCO), 04 Nov. 2003.